Gas Phase Axial Mixing at Extremely High Irrigation Rates in a Large Packed Absorption Tower

Extensive gas phase dispersion data are reported for extremely high liquid-gas ratios in a cylindrical packed absorption tower operated at atmospheric pressure under counterflow conditions.

The dispersion data report gas Peclet numbers in terms of superficial liquid and gas Reynolds numbers over the range

$$0 < NRe_L < 1500$$

$$15.0 < NRe_S < 500$$

An increase in Peclet number with increasing gas rate is observed at subloading conditions.

Reverse gas flow was observed in the gas phase when the liquid Reynolds number exceeded 650. Dispersion in the gas phase at liquid rates for which $NRe_L < 650$ is consistent with previously recorded correlations but becomes independent of further increases of liquid rate when NRe_L is > 650.

The dispersion coefficients obtained by dynamic testing under reverse gas flow conditions were consistent with those obtained from steady state absorption profiles and provide a quantitative explanation for the anomalies in plug-flow K_{La} at high water rates recorded by Sherwood and Holloway (1940).

EDWARD T. WOODBURN

Department of Chemical Engineering
University of Natal
Durban, South Africa

SCOPE

Under normal operating conditions in a packed absorption tower, the axial dispersion of a solute in the gas phase is small and its effect on absorption tower performance may be neglected (Brittan and Woodburn, 1966).

For the physical absorption of sparingly soluble gases, however, extremely high liquid-gas ratios are necessary and existing correlations indicate that under these conditions the dispersive effect in the gas may well become significant.

No dispersion data has however hitherto been reported in the relevant flow regions and as the low water rate correlations (Dunn et al., 1962; de Maria and White, 1960; Sater and Levenspiel, 1966) when extrapolated show mutual inconsistencies of several orders of magnitude, it has not been previously possible to assess the interaction between mass transfer and dispersion precisely.

In addition to providing a basis for the understanding of mass transfer anomalies reported by Sherwood and Holloway (1940) and Cooper et al. (1941), the operation of absorbers under these conditions provides an experimental justification for the general use of dispersion parameters obtained by dynamic testing procedures in the prediction of steady state absorber performance.

Miyauchi and Vermeulen (1963) have shown that the effect of axial dispersion in one phase, of a two-phase continuous flow system, will manifest itself as an inlet discontinuity in the solute profile. Although this prediction is a consequence of an idealized model and cannot be expected to exist physically, Brittan (1967) has shown how it may be used with a knowledge of the experimental profile of the solute to estimate axial dispersion under steady state conditions.

The axial dispersive effects in the gas phase have been determined over a wide range of both liquid and gas flow rates using dynamic testing with ^{85}Kr as a tracer. This data can be compared with a limited amount of information relating to the effect of axial dispersion on experimentally determined steady state CO_2 profiles in the gas phase inside the same tower. The absorption of CO_2 was performed at atmospheric temperature and pressure with water as solvent.

Finally, in accordance with the observations of Mellish (1968), attention was paid to liquid-gas interactions. This was done by recording experimental pressure gradients in the gas phase as a function of liquid and gas flow rates, with a view to establishing the presence of loading. In addition, some measurements by which macro-scale reverse gas flow was detected at high liquid rates were done.

CONCLUSIONS AND SIGNIFICANCE

All experimental data refer to a cylindrical absorption tower 0.292 m in internal diameter, packed to a depth of 10.97 m, with 0.025 m stoneware Raschig rings, and with a fractional void volume of 0.714.

1. Over the range

$$15.0 < NRe_S < 500$$

$$126 \leq NRe_L < 1321$$

increases in the superficial gas rate (at constant liquid rate) are associated with increases in the axial Peclet number in the gas phase.

2. The data are consistent with a power law dependence of the axial dispersion coefficient on the gas pore velocity, for example,

$$E_G \alpha U_G^n$$

where the exponent n is > 1.0 for loading conditions and lies in the range $0 \leq n \leq 1.0$ for subloading conditions.

3. The form of the correlation proposed by de Maria and White (1960), Sater and Levenspiel (1966), and Dunn et al. (1962) for the dependence of axial gas phase dispersion on liquid rate at constant gas rate is confirmed for liquid rates at which $NRe_L < 650$.

4. Over the range $650 < NRe_L < 1500$, the axial dispersion in the gas phase is independent of the liquid rate.

5. For liquid rates in the range $650 < NRe_L < 1500$, reverse gas flow induced by the counterflowing liquid was measured.

6. From the two former conclusions, it is reasonable to infer that an additional dispersive mechanism associated with reverse gas flow becomes operative at $NRe_L \geq 650$.

This is potentially significant in relating dispersion effects to mass transfer anomalies if the new dispersion mechanism can be correlated with backmixing in the gas phase.

Buchanan (1971) has observed that only backmixing significantly affects estimates of mass transfer coefficients. This manifests itself in steady state absorption profiles where the inlet solute discontinuity, which is uniquely sensitive to the Peclet number, can only be generated by backmixing.

7. A limited number of experimental steady state gas solute profiles obtained for $NRe_L > 650$ gave estimates of Peclet numbers which are consistent with those obtained by dynamic testing.

The mass transfer coefficients which were estimated simultaneously do not show the anomalous decrease with increase in water rate observed for $NRe_L > 750$ by Sherwood and Holloway (1940).

The axial dispersion of a solute in a gas flowing through a packed bed has been extensively studied. There have been fewer experimental investigations of this type of dispersion in irrigated packed beds. Of these the work of Kramers and Alberda (1953), Dunn et al. (1962), de Maria and White (1960), Sater and Levenspiel (1966) are the most relevant. In addition, some information in this context has been reported by de Waal and van Mameren (1965).

A satisfactory model for dispersion should contain parameters which can be determined independently of the dispersion measurement and should have predictive capabilities in absorption and other steady state mass transfer situations.

It is also desirable that the techniques used to describe dry bed dispersion should extrapolate to the prediction of dispersion in irrigated beds. The obvious way to do this is to link a model of the bed structure to the gas dispersive effects.

The simplest postulate which can be made is the series-of-stirred cells model for which, by identifying a packing element as being equivalent to the dimension of a unit cell, McHenry and Wilhelm (1957) showed for dry beds that the limiting value of the Peclet number was 2.0.

For irrigated beds, however, experimental data is reported as the H.M.U. of a typical cell without attempting to link this parameter with the flow within the bed.

Turner (1958, 1959), formulated more sophisticated bed structure models and his work has recently been extended by Buffham et al. (1970). Recently Gunn and co-workers have published a series of papers (Gunn, 1969; Gunn and Pryce, 1969; England and Gunn, 1970; Gunn, 1971) in which the effect of bed structure on dispersion has been closely examined.

The bulk of the experimental information on irrigated beds is, however, available in the form of a simple one-dimensional continuum model in which the dispersive effect is characterized by an axial dispersion coefficient E_G or its associated dimensionless group $NPe_G = U_G d_p / E_G$.

Little attempt has been made to correlate E_G with local variations in gas velocity, as suggested by Saffman (1959), in view of the lack of knowledge associated with the small-scale flow patterns.

STEADY STATE ABSORPTION PROFILE

Miyauchi and Vermeulen (1963) have incorporated the axial dispersion coefficient in the prediction of steady state mass transfer in continuous two-phase flow systems. Brittan (1967) has extended their general treatment based on linear systems to the nonlinear equations describing the physical absorption of a solute present in significant amounts.

The justification for the use of the axial dispersion coefficient for the prediction of steady state solute profiles appear to be based on the acceptance of the Fickian analogy with the molecular diffusion coefficient, which implies effectively backmixing.

The use of the axial dispersion coefficient to generate a steady state gas solute profile $f(\eta)$ has been described by Brittan (1967). The following differential equation is an extension of his treatment (Woodburn, 1972) and reduces Brittan's differential equation if $\Delta\pi$ is set to zero:

$$\frac{\partial^2 f}{\partial \eta^2} + \frac{y^0}{(1 - y^0 f)} \left(\frac{\partial f}{\partial \eta} \right)^2 - \left(\frac{P}{(1 - y^0 f)} + \frac{\Delta\pi}{(1 - y^0 f)(1 + \Delta\pi(1 - \eta))} + N \right) \frac{\partial f}{\partial \eta} - \frac{PNA}{F} \times \frac{(1 + \Delta\pi(1 - \eta))}{(1 + \Delta\pi)} \times \frac{(1 - y^0 f)}{(1 - y^0)} \times \left(f - \frac{m(1 + \Delta\pi) F v^0_{CO_2} x^1}{(1 + \Delta\pi(1 - \eta)) v_{H_2O} y^0} \right) + PN(1 - y^0 f) \times \left(\frac{f}{(1 - y^0 f)} - \frac{f^1}{(1 - y^0 f^1)} \right) + \frac{N\Delta\pi f}{(1 + \Delta\pi(1 - \eta))} - \frac{\Delta\pi^2 f}{(1 + \Delta\pi(1 - \eta))^2} = 0 \quad (1)$$

It is of interest to note in this formulation the high degree of interdependence of the dispersion group

$$P = \frac{U_G Z}{E_G}$$

and the number of transfer units

$$N = \frac{k_L a Z}{U_L}$$

For small pressure gradients, the two groups appear almost symmetrically in Equation (1). This confirms the

reasonableness of using essentially the product PN to characterize the profile and illustrates the difficulty of estimating the groups individually from the profile.

However, the boundary conditions provide a sensitive relation for P, namely,

$$\text{At} \quad \text{(i)} \quad \eta = 1.0 \qquad \frac{\partial f}{\partial \eta} = 0$$

$$\text{(ii)} \quad \eta = 0.0 \qquad \left(\frac{1 - f_0}{1 - y^0}\right) = -\frac{1}{P}\left(\frac{\partial f_0}{\partial \eta} - \frac{f_0 \Delta\pi}{1 + \Delta\pi}\right)$$

The latter condition results from a mass balance for the solute in the gas phase at the inlet to the tower, assuming no axial dispersion in the gas supply pipe.

A least squares procedure was used over all the experimental points on a steady state profile to find the best value of N. N was constrained to lie between an upper bound equal to the Sherwood and Holloway extrapolation and a lower bound corresponding to the experimental plug flow estimate.

As the Peclet number had to be solved implicitly for each value of N (in order to match the value used to compute the profile with the inlet boundary condition), the data processing involved one regression procedure within another.

The iterative procedure for the determination of P used the Newton approximation at the $\eta = 0$ boundary with the partial differential coefficients required being carried through the Runge-Kutta-Gill procedure used to generate $f(\eta)$, in the manner described by King (1967), with initial values at $\eta = 1$.

DYNAMIC TESTING

The bulk of the dispersion data was obtained using a dynamic testing procedure similar to those described by Hougen and Walsh (1961). This procedure involved determining the concentrations of tracer $C_1(t)$ and $C_2(t)$ at two points within the bed located at distances z_1 and z_2, respectively, from the gas inlet and following the injection of an imperfect pulse of tracer into the gas stream upstream of both detection positions.

For a linear system the two experimental concentrations are related to each other through the convolution integral and the system impulse response

$$C_2(t) = \int_0^\infty C_1(\tau) h(t - \tau) d\tau$$

where

$$h(t) = \frac{(z_2 - z_1)}{2(\pi E_G t^3)^{1/2}} \exp - \frac{((z_2 - z_1) - U_G t)^2}{4E_G t} \quad (2)$$

With $C_1(t)$ and $C_2(t)$ being available experimentally, the best values of U_G and E_G were obtained by a nonlinear least squares procedure using the convergence procedures described by Law and Bailey (1963).

EXPERIMENTAL DESIGN

Three sets of experimental measurements were taken:

1. Measurement of axial dispersion in the gas using dynamic testing procedures.
2. Measurement of gas pressure drops, reverse gas flow, and dynamic liquid hold-ups under conditions corresponding to those of the dynamic testing.
3. Measurement of the steady state gas solute profile within the tower under physical absorption conditions.

EXPERIMENTAL APPARATUS AND PROCEDURES

Absorption Column

The absorption tower was cylindrical with an internal diameter of 0.292 m and a packed height of 10.97 m. The shell of the tower was made of stainless steel and was packed with randomly dumped 0.025-m stoneware Raschig rings.

Irrigating water was added to the top of the tower via a four-point nozzle distributor, and wall-wiper redistributor rings were located 3.05 m and 6.10 m above the bottom of the column.

At the bottom of the column the gas inlet was located centrally as a 0.025-m diam. pipe which passed through the bottom packing support into the packing. The free space under the packing support was a very shallow cone. The position of the liquid interface could be observed by a boiler sight glass and was maintained just below the packing support.

Dispersion Measurements

Dispersion measurements followed the general pattern of detecting a radioactive tracer injected at an upstream position as an impulse at two detection points located within the bed.

The detection points consisted of a hollow sheath with lateral windows stretching across the column diameter. It was possible to fit inside these sheaths Anton type 108 C G-M counters. These detectors are robust and comparatively small (0.0159 m in diameter and with an overall length of 0.19 m). Careful precautions were taken to minimize the possibility of tracer being trapped between the detector and its protective sheath. As the O.D. of the outer sheath was less than that of a packing piece, it was felt that the disturbance to the packing caused by the detector assembly would not seriously affect the bed structure.

Detection points (which could also be used for pressure tappings, and gas solute sample points) were located respectively 0.914 m, 2.742 m, 4.570 m, 6.398 m, 8.226 m, 10.054 m above the bottom of the packing. For the bulk of the dispersion runs isotope was injected in the gas feed pipe immediately before it entered the packing, with the counters located at the 0.914 m and 8.24 m detection points, respectively. Some earlier runs were done in which the isotope was injected at a central point within the bed, but this was abandoned in the later runs because of the uncertainty of the completeness of the radial dispersion of the tracer.

The tracer used was ^{85}Kr which is primarily a β-emitter and is only sparingly soluble in water. As the range of β-particles in air is extremely limited and as the counters have a low γ and Brämstrahlung efficiency, the isotope detected would be largely within 1 cm of the GM tubes, and thus the detectors would effectively measure axial dispersion.

The radioactive disintegrations after pre-amplification and pulse-shaping were recorded individually on an analogue tape recorder (Phillips Ana-Log) and processed subsequently on to an IBM 024 card-punch using twin printing scalers (PW 4230) as an intermediate buffer. The data was then available on punched cards in a suitable form for computer input. This enabled sampling frequencies of 5 kHertz to be achieved.

Pressure-Drop Measurements

Simple hollow probes fitting inside the detection sheaths described for the dispersion measurements were used for pressure tappings. Air was blown slowly through these probes into the column and the differential pressure for the flushing air was recorded on either an inclined or a vertical water manometer.

The pressure probes were located at the 0.914 m and the 10.054 m detection point, respectively.

Dynamic Hold-Up Measurements

These were done by simultaneously shutting off the inflowing water and at the same time allowing the column contents to drain for approximately 15 min. into a weighed receiver. The hold-ups recorded in this way were approximately 90% of the values anticipated from the Otake-Okada (1953) correlation.

CO_2 Analysis

Gas sample probes were located in the detection points described for the dispersion runs. In addition, the feed gas (0-m)

and the exit gas (10.97 m) were also sampled. Special purpose gas sample probes were inserted in the bed near the inlet at 0.228 m and 0.457 m.

The sample probes located at the detection stations could sample from three different radial positions. Normally 10 axial positions were sampled with two radial positions at 0.914 m and 4.570 m. A typical steady state absorption run would involve continuous withdrawal of 12 samples at rates of approximately 50 ml m^{-1} and a sequential analysis of the samples in a fixed order on a gas chromatograph.

The chromatograph was extremely simple and cheap to construct using as a stationary phase water adsorbed on Poropak T. With a permanent gas such as CO_2, the column could operate at atmospheric temperature, and the effect of ambient temperature fluctuations was minimized by using high filament currents in the thermal conductivity detector.

The GC provided well-defined CO_2 peaks with stable base-lines. The sequential analysis was controlled by a Camtimer based on an individual analysis time of 1¼ min. The scan time for a 12-point profile was 15 min. and because usually 5 to 6 repetitive scans were done, the column was required to operate steadily for 1½ hours for a particular run.

The principal experimental difficulty was associated in the withdrawal of gas samples in the presence of large amounts of counterflowing liquid. If water is entrained in the gas sample, then the possibility of absorption within the probe exists.

The problem of minimizing the amount of entrained water in the gas samples was partly solved by locating the sample probe within the sheath immediately under the top of the sheath. It was hoped that water would drain away through the lateral windows. However, some water was observed in the gas samples, and small separators were fitted to the probes where they emerged from the column.

A small amount of entrained water may be tolerated for sparingly soluble gases as it will become saturated without affecting the bulk composition of the gas significantly. On this basis the gas sample rate was maintained at 50 ml m^{-1} which was greatly in excess of the volume of entrained water.

RESULTS

Data Processing

All the results showed that a considerable scatter existed within the Peclet numbers. In general, the experimental data were well described by Equation (2) in Woodburn (1972), although some non-Gaussian features were present.

Analysis of the data processing procedure has shown that while confidence limits of 5% are associated with the estimates of U_G, the corresponding limits for E_G are about 30%. This increased uncertainty in E_G appears to originate in the deviations in the experimental curves from the Gaussian form assumed in Equation (2).

All the experimental curves exhibit non-Gaussian features such as a sharp initial break-away and a slow final return. The deviations in U_G and E_G are compounded by recording them as the ratio $U_G dp/E_G$ since a small negative correlation ($r = 0.5$) has been detected in the data processing between U_G and E_G.

Axial Dispersion from Dynamic Testing—Dry Beds

A large amount of runs on dry packings were done to assess the validity of the technique and a mean $NPe_G \doteq 1.0$ was recorded.

This is in conflict with the prediction of $NPe_G = 2.0$ of McHenry and Wilhelm (1957) which was obtained for glass spheres. Other workers too (Evans and Kenney, 1966; Gunn and Pryce, 1969) have confirmed these results for spheres. There is some indication (Dunn et al., 1962) that for Raschig rings and saddles Peclet numbers in the range 0.6 to 0.2 are appropriate. De Maria and White's (1960) results on wetted packing at zero water rate show also Peclet numbers in this range.

Axial Dispersion from Dynamic Testing—Irrigated Beds

In Fig. 1 experimental dispersion data are summarized as plots of log NPe_G vs. log NRe_S at constant values of NRe_L. Also plotted are

1. An approximate representation for the dependence of log NPe_G on log NRe_S for dry beds (compare Gunn and Pryce, 1969; Edwards and Richardson, 1968).

2. The dependence of log NPe_G on log NRe_S for values of $NRe_L = 126, 252, 379$, respectively, in terms of the correlation of Dunn et al. (1962), namely,

$$NPe_G = \frac{a_t d_p}{6(1-\epsilon)}(0.665 - 1.90 \times 10^{-4} NRe_S) \times 10^{-1.13 \times 10^{-3} NRe_L}$$

This correlation is particularly relevant to this work as it included similar size packing and is valid of the ranges

$$600 \leq NRe_S \leq 2200$$

$$0 \leq NRe_L \leq 375$$

Examination of the figure shows that in the region where the two investigations overlap, namely, at $NRe_S = 600$, the value of NPe_G reported in this work is only half of that of Dunn et al. In the light of the observations relating to the variation of the Peclet number in dry beds, this discrepancy is probably not significant and may reflect the differences in dynamic testing procedures.

In order to facilitate the interpretation of dispersion data in terms of gas-liquid flow characteristics, a 400

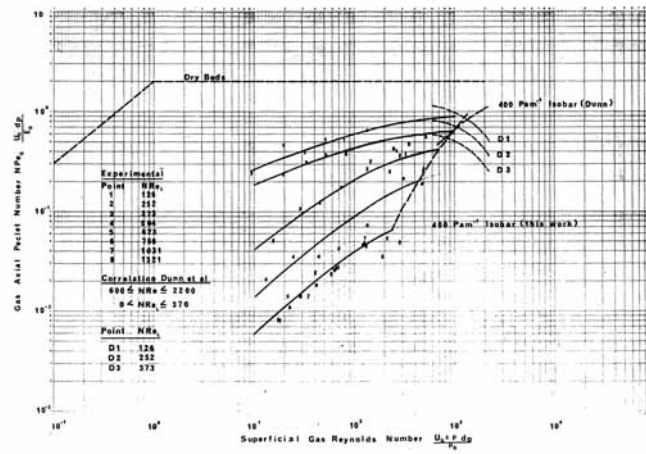

Fig. 1. Summary of experimental dispersion data.

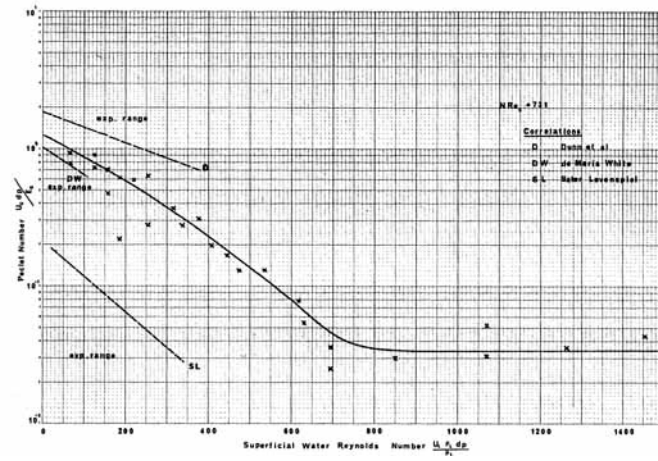

Fig. 2. Dependence of Gas-phase axial mixing on liquid rate at a constant gas Reynolds of 73.1.

Pa m^{-1} contour has been plotted on the dispersion data. This corresponds approximately with the onset of loading (Treybal, 1968) although Leva (1953) reports lower values and Ramm (1968) cites 600 Pa m^{-1}. The relevant pressure gradients were those determined experimentally and are reported on Figure 3.

A similar 400 Pa m^{-1} contour was plotted on the Dunn et al. correlations using the pressure-gradient data of Leva (1953).

The experimental range of operations of some previous investigators are shown in Table 1.

In Table 2 the gas Reynolds number, at which a pressure gradient of 400 Pa m^{-1} occurs, is reported for a given liquid rate in terms of

1. Experimental observations in this work.
2. Predictions using the graphical correlation of Leva (1953).

It will be seen that while the bulk of the dispersion work in this investigation was carried out at pressure gradients less than 400 Pa m^{-1}, it is likely that the pressure gradients considerably exceeded this figure in investigations of Dunn et al.

Furthermore, reported inconsistencies in the work on 0.0125-m rings between de Maria and White (1960) and Sater and Levenspiel (1966) may have arisen from the fact that while the former work was done at subloading, the latter was almost certainly done in the high loading regions.

In order to facilitate comparison between this work and that of Dunn et al., it is helpful to consider a power law dependence between E_G and U_G of the form of that proposed for dry beds by Scheidegger (1957) and Harleman and Rumer (1963), namely,

$$E_G = MU_G^n$$

which leads to the expression

$$\log NPe_G = (1 - n) \log NRe_G + \text{Constant}$$

This provides a basis for the plot on Figure 1 from which changes in slope are associated with changes in the exponent n.

At very low gas rates, $n \rightarrow 0$ and the gas phase dispersion is dominated by changes in liquid rate. At gas rates consistent with the onset of loading $n \rightarrow 1.0$ and at higher rates it becomes larger and the familiar negative exponent on the $NRe_S - NPe_G$ relationship will be observed. It must be emphasized, however, that the negative exponent reported by de Maria and White (1960) is not consistent with this postulate.

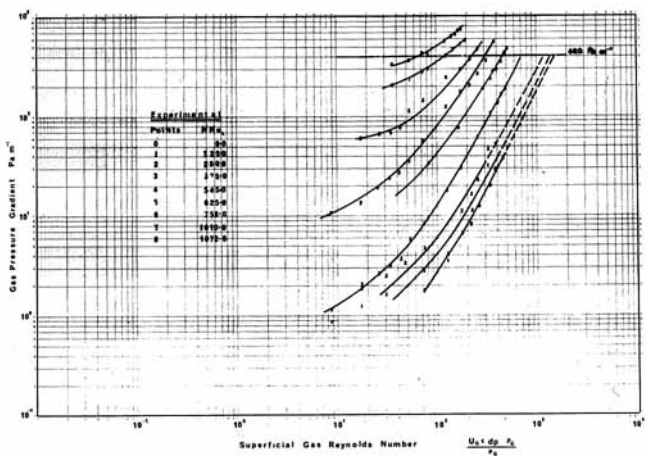

Fig. 3. Pressure gradients constant liquid rate.

Table 1. Experimental Range of Previous Investigators

	Packing size	NRe_L	NRe_S
Dunn et al. (1962)	0.025m	0-375	600-2200
de Maria and White (1960)	0.0125m	0-107	18.6-126
Sater and Levenspiel (1966)	0.0125m	20-340	50-580

Table 2. Gas Reynolds Number Associated with a Pressure-Gradient of 400 Pa m^{-1}

NRe_L	NRe_S Experimental	NRe_S from correlation 0.025-m rings	0.0125-m rings
126	1,250	1,350	200
252	1,000	1,050	75
379	660	800	—
504	480	625	—
632	310	450	—
758	230	325	—
1,010	125	—	—
1,072	70	—	—

The power-law dependence of E_G on U_G is consistent with the correlations of Dunn et al. although the exponent n tends to a value of 1.0 at pressure gradients of about 200 Pa m^{-1}.

Figure 2 shows the dependence of gas-phase axial mixing on liquid rate at a constant gas Reynolds number of 73.1. Other runs in this series are available for NRe_S = 36.5, 124, 148.5, 220.

This data is not cross-plotted from Figure 1 but is an earlier series carried out at constant gas rate and in which there were variations in the positions of the injection and detection points and in the data processing equipment (Woodburn, 1972).

The data for NRe_S = 73.1 was the most complete set available, with three of the other four runs consistent with it, all showing a break-point at $NRe_L \doteqdot 650$.

The run at NRe_S = 220 was an exception as no dispersion data are recorded in excess of NRe_L = 750, at which point the column no longer operated stably.

INDUCED REVERSE GAS FLOW

Experiments were performed in which the gas inlet was disconnected and a rotameter fitted in what was previously the gas discharge pipe at the top of the column. Under these conditions, any gas flow recorded could only be that induced by the down-flowing water.

The mechanism by which the air flow is caused is not clear but may well be associated with entrainment of air by water flowing in the region of the wall.

The onset of this reverse gas flow was detected at a liquid Reynolds number of 685.

Its presence may also be inferred from Figure 4, on which the pressure gradient at zero superficial gas flow is recorded as a function solely of liquid rate. It is clear from Figure 4 that there is also a significant dependence of pressure gradient on water rate at nonzero superficial gas rates.

Although the conditions associated with reverse gas flow are probably specific to this column, it is of interest to note that Uchida and Fujita (1937) recorded sucking to start at a liquid rate of 100 $m^3m^{-2}hr.^{-1}$ (equivalent to NRe_L = 694 on this column). Their work was done on

comparable packing with smaller bed depths (max. 3.2 m).

Broz and Kolar (1969) have also recorded gas pressure gradients as a function of liquid rate for 10-mm glass spheres in a 0.19-m diameter column with a bed depth of 1.10 m. Pressure gradients were detected at liquid rates greater than 13 kg $m^{-2}s^{-1}$. (Volumetric flux of 46.8 $m^3m^{-2}hr^{-1}$.)

The potential significance of a flow of air induced in the concurrent direction by the down-flowing water in the presence of a superficial net upflow of air is that it suggests a mechanism by which backmixing can occur.

Buchanan (1971) has clearly distinguished between the various dispersion mechanisms which are detected by dynamic testing procedures and has shown that of these only the backmixing contribution is likely to be of significance in the estimation of mass transfer coefficients.

In this context it may be fortuitous to note that in the classic paper of Sherwood and Holloway (1940) the onset of anomalous deviations for Raschig rings in the power-law dependence of K_{La} on liquid rate was noted at 18,000 lb hr^{-1} ft ($NRe_L = 610$).

It is perhaps reasonable to infer from the dispersion data reported in Figures 1 and 2 that an additional dispersion mechanism becomes operative in the region $NRe_L = 650$, at which point the gas Peclet number as inferred from dynamic testing is no longer sensitive to further increases in liquid rate.

The experimental results for induced reverse gas flow in this column are correlated by the following relationship:

$$NRe_{RF} = 131.5 \log_{10} NRe_L - 370.4$$

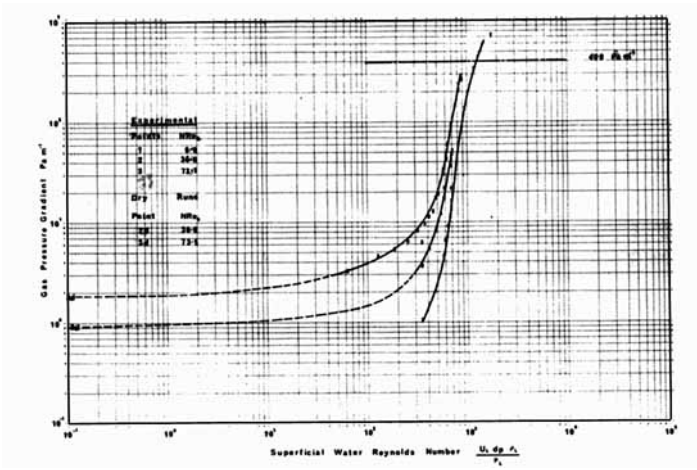

Fig. 4. Pressure gradients constant gas rate.

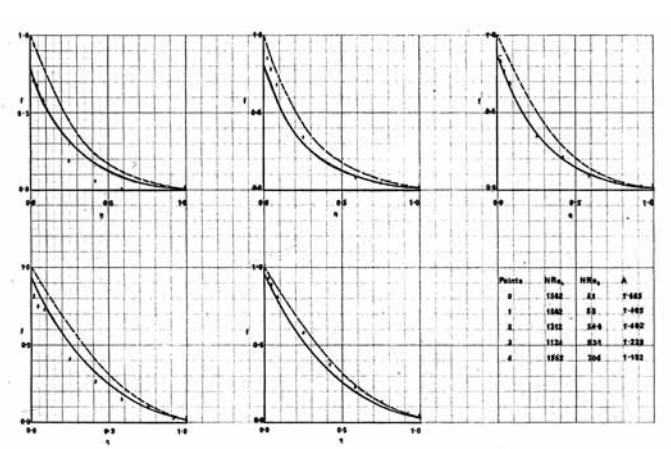

Fig. 5. Five sets of experimental absorption profiles.

Table 3. Data from Absorption Profile

(i) Mass transfer correlation using Sherwood and Holloway (1940) relationships.
(ii) Plug flow coefficient estimated from experimental profiles not terminal conditions.
(iii) Regressed coefficient estimated from Equation (1).

$\frac{U_L}{mU_S^0}$	NRe_L	NRe_S	Mass transfer coefficients: Correlation (i) hr^{-1}	Plug flow (ii) hr^{-1}	Regression (iii) hr^{-1}	NPe_G
1.685	1,562	51.0	374	90.6	234.2	0.024
1.405	1,560	53.1	374	101.3	239.0	0.031
1.402	1,311	54.6	326	125.4	326.0	0.035
1.238	1,124	53.1	290	134.0	290.0	0.051
1.152	1,560	70.5	374	144.0	262.0	0.082
1.101	1,437	70.8	354	153.0	253.5	0.123
1.022	1,312	70.6	326	122.0	225.0	0.069

STEADY STATE ABSORPTION PROFILES

Five sets of experimental profiles are shown in Figure 5 together with profiles computed according to Equation (1) using a mass transfer coefficient giving the closest fit to the experimental data. The computed Peclet numbers associated with each profile are tabulated in Table 3 as is the apparent mass transfer coefficient based on the assumption of plug flow in both phases.

In all cases the plug flow profile (shown dotted on Figure 5) lies above that generated using the axial dispersion coefficient (shown as a full line). The regressed lines are in fair agreement with the experimental data, and the recorded values for the Peclet number are consistent with those predicted by dynamic testing.

The mass transfer coefficients, while significantly greater than those inferred using the assumption of plug flow, are still less than would be predicted from the Sherwood and Holloway correlation.

The experimental data reported by Sherwood and Holloway show a deviation from their power-law correlation beginning at $NRe_L = 610$ with a maximum $K_{La} = 200$ hr^{-1} recorded at $NRe_L = 750$.

In conclusion it may be said:

1. That under conditions which are associated with reverse gas flow, the gas-phase axial mixing coefficient inferred by dynamic testing is consistent with that inferred from the steady state absorption profile.

2. The onset of measurable reverse gas flow in this column occurred at $NRe_L \doteq 650$ at which value the gas-phase axial dispersion coefficient determined by dynamic testing became independent of further increases in liquid rate at constant gas rate.

This suggests the onset of a new dispersion mechanism in the gas which may reasonably be imputed to backmixing.

ACKNOWLEDGMENTS

The author wishes to acknowledge the financial assistance of the CSIR and Atomic Energy Board for capital and running expenses.

NOTATION

A = absorption factor U_L/mU_s^0
a_t = packing surface per unit volume of tower, m^{-1}
$c(t)$ = experimental tracer concentration, mcm^{-3}
dp = characteristic size of packing, m
E_G = axial dispersion coefficient in gas phase, m^2s^{-1}

F = correction factor = $(273 + T)/(273 + T^0)$
$f, f(\eta)$ = dimensionless gas solute volume fraction = y/y^0
$h(t)$ = system impulse response, s^{-1}
HMU = height of Mixing Unit = $2dp/NPe_G$, m
k_La = liquid film mass transfer coefficient assumed ≡ overall mass transfer coeff., s^{-1}
m = equilibrium constant m = $\frac{y}{x}\frac{v_{H2O}}{v_{CO_2}}$
N = number of transfer units = k_LaZ/U_L
n = exponent in relationship $E_G\alpha U_G^n$
NRe_L = liquid Reynolds number = $U_L\rho_L dp/\mu_L$
NRe_S = gas Reynolds number = $U_G\rho_G dp\epsilon/\mu_G$
NPe_G = gas axial Peclet number, $U_G dp/E_G$
P = gas axial Peclet number based on overall bed depth, U_GZ/E_G
$\left(-\frac{\Delta p}{\Delta z}\right)$ = pressure gradient in axial direction in gas phase, Pa m^{-1}
t = time, s
U_G = gas 'pore' velocity estimated from regression, ms^{-1}
U_L = volumetric flux water (based on superficial tower X-section), $m^3m^{-2}s^{-1}$
U_S = volumetric flux gas (based on superficial tower X-section), $m^3m^{-2}s^{-1}$
v_{CO_2} = specific volume CO_2 in gas-phase, $m^3kgmole^{-1}$
v_{H_2O} = specific volume water in liquid phase, $m^3kgmole^{-1}$
x = volume fraction CO_2 in liquid
y = volume fraction of CO_2 in gas phase
z = axial position in bed measured from gas inlet, m
Z = overall depth of packing, m

Greek Letters

ϵ = fractional void volume in bed
η = dimensionless length coordinate = z/Z
μ = fluid viscosity, Nsm^{-2}
$\Delta\pi$ = pressure drop over bed normalized w.r.t. to ambient atmospheric pressure
ρ = fluid density, kgm^{-3}
τ = dummy time variable in convolution integral, s

Subscripts

0 refers to fluid condition immediately downstream of gas inlet to column
1, 2 refers to conditions within the bed with point 1 being closer to gas inlet
G = gas
L = liquid

Superscripts

0 refers to fluid conditions immediately upstream of gas inlet to column
1 refers to fluid conditions immediately downstream of gas exit from column

LITERATURE CITED

Brittan, M. I., "The simultaneous determination of axial dispersion and mass transfer coefficients," *Chem. Eng. Sci.*, **22**, 1019 (1967).

Brittan, M. I., and E. T. Woodburn, "The Influence of Axial Dispersion on Carbon Dioxide Absorption Tower Performance," *AIChE J.*, **12**, 541 (1966).

Broz, Z., and V. Kolar, "Two-phase counter current flow through a bed of packing," *Coll. Czech. Chem. Comm.*, **33**, 349 (1968).

Buffham, B. A., L. G. Gibilaro, and M. N. Rathor, "A Probabilistic Time Delay Description of Flow in Packed Beds," *AIChE J.*, **16**, 218 (1970).

Cooper, C. M., R. J. Christl, and L. C. Peery, "Packed Tower Performance at High Liquor Rates," *Trans. Am. Inst. Chem. Engrs.*, 37, 979 (1941).

de Maria, F., and R. M. White, "Transient Response of Gas Flowing Through Irrigated Packing," *AIChE J.*, **6**, 473 (1960).

de Waal, K. J. A., and A. L. van Mameren, "Pressure Drop, Liquid Hold-up and Distribution, Residence Time Distribution and Interfacial Area Between Gas and Liquid in One Packed Column," *AIChE—I. Chem. E. (Symp. Ser.)*, **6**, 6 (1965).

Dunn, W. E., et al., "Longitudinal mixing in packed gas-absorption columns," Univ. of Calif. Lawr. Rad. Lab., UCRL 10394 (1962).

Edwards, M. F., and J. F. Richardson, "Gas disperson in packed beds," *Chem. Eng. Sci.*, **23**, 109 (1968).

England, R., and D. J. Gunn, "Dispersion, pressure drop and chemical reaction in packed beds of cylindrical particles," *Trans. Inst. Chem. Eng. (London)*, **48**, T265, (1970).

Evans, E. V., and C. N. Kenney, "Gaseous dispersion in packed beds at low Reynolds numbers," *Trans. Inst. of Chem. Eng. (London)*, **44**, T189 (1966).

Gunn, D. J., "Axial dispersion in packed beds: The effect of the quality of the packing," **47**, 109 (1971).

———., "Theory of Axial and Radial Dispersion in Packed Beds," *Trans. Inst. of Chem. Eng. (London)*, **47**, T351 (1969).

———., and C. Pryce, "Dispersion in packed beds," *ibid.*, T341.

Harleman, D. R. F., and R. R. Rumer, "Longitudinal and lateral dispersion in an isotropic porous media," *J. Fluid Mech.*, **16**, 385 (1963).

Hougen, J. O., and R. A. Walsh, "Pulse testing method," *Chem. Eng. Progr.*, **57**, 69 (1961).

Kramers, H., and G. Alberda, "Frequency response analysis of continuous flow systems," *Chem. Eng. Sci.*, **2**, 173 (1953).

King, R. P., "Estimation of parameters in systems defined by differential equations," *South African. J. Sci.*, **63**, 91 (1967).

Law, V. J., and R. V. Bailey, "A method for the determination of approximate system transfer functions," *Chem. Eng. Sci.*, **18**, 189 (1963).

Leva, M., "Tower packings and packed tower design," United States Stoneware Co., Akron, Ohio, 40 (1953).

Lubin, B., "A study of flow rates in a twenty-four inch packed tower," Ph.D. thesis, Univ. of Missouri, Rolla (1949).

McHenry, K. W., Jr., and R. H. Wilhelm, "Axial Mixing of Binary Gas Mixtures Flowing in a Random Bed of Spheres," *AIChE J.*, **3**, 83 (1957).

Mellish, W. G., "Applicability of Dispersion results to packed columns," *ibid.*, **14**, 668 (1968).

Miyauchi, T., and T. Vermeulen, "Longitudinal dispersion in two-phase continuous flow operations," *Ind. Eng. Chem. Fundamentals*, **2**, 113 (1963).

Otake, T., and K. Okada, "Liquid hold-up in packed towers; operating hold-up without gas flow," *Kagaka Kogaku*, **17**, 176 (1953).

Ramm, V. M., "Absorption of Gases," Israel program for Sci. Trans., 342 (1968).

Saffman, P. G. "A theory of dispersion in a porous medium," *J. Fluid Mech.*, **6**, 321 (1959).

Sater, V., and O. Levenspiel, "Two-phase flow in packed beds," *Ind. Eng. Chem. Fundamentals*, **5**, 86 (1966).

Scheidegger, A. E., "On the theory of flow of miscible phases in porous media," Compt. Rend. Ass. Gen. Toronto, *Ass. Int. Hydrol. Sci.*, **2**, 236 (1957).

Sherwood, T. K., and F. A. L. Holloway, "Performance of Packed Towers—Liquid Film Data for Several Packings," *Trans. Am. Inst. Chem. Engrs.*, **36**, 39 (1940).

Turner, G. A., "The flow structure in packed beds. A theoretical investigation utilizing frequency response," *Chem. Eng. Sci.*, **7**, 156 (1958).

———., "The frequency response of some illustrative models of porous media," *ibid.*, **10**, 14 (1959).

Treybal, *Mass Transfer Operations*, p. 161, McGraw Hill, New York (1968).

Uchida, S., and S. Fujita, "Irrigated Packed Towers I—V," *J. Soc. Chem. Ind. (Japan)*, **39**, 432B (1936).

———., "Irrigated Packed Towers VI-VIII," *ibid.*, **40**, 238B (1937).

Woodburn, E. T., "A study of gas-phase Axial Mixing in a Packed Absorption Tower" Ph.D. thesis, Univ. Witwatersrand, Johannesburg (1972).

Manuscript received January 28, 1974; revision received June 25 and accepted June 26, 1974.